

# Aerosol–Ice Formation Closure

## A Southern Great Plains Field Campaign

D. A. Knopf, K. R. Barry, T. A. Brubaker, L. G. Jahl, K. A. Jankowski, J. Li, Y. Lu, L. W. Monroe, K. A. Moore, F. A. Rivera-Adorno, K. A. Saucedo, Y. Shi, J. M. Tomlin, H. S. K. Vepuri, P. Wang, N. N. Lata, E. J. T. Levin, J. M. Creamean, T. C. J. Hill, S. China, P. A. Alpert, R. C. Moffet, N. Hiranuma, R. C. Sullivan, A. M. Fridlind, M. West, N. Riemer, A. Laskin, P. J. DeMott, and X. Liu

**ABSTRACT:** Prediction of ice formation in clouds presents one of the grand challenges in the atmospheric sciences. Immersion freezing initiated by ice-nucleating particles (INPs) is the dominant pathway of primary ice crystal formation in mixed-phase clouds, where supercooled water droplets and ice crystals coexist, with important implications for the hydrological cycle and climate. However, derivation of INP number concentrations from an ambient aerosol population in cloud-resolving and climate models remains highly uncertain. We conducted an aerosol–ice formation closure pilot study using a field-observational approach to evaluate the predictive capability of immersion freezing INPs. The closure study relies on collocated measurements of the ambient size-resolved and single-particle composition and INP number concentrations. The acquired particle data serve as input in several immersion freezing parameterizations, which are employed in cloud-resolving and climate models, for prediction of INP number concentrations. We discuss in detail one closure case study in which a front passed through the measurement site, resulting in a change of ambient particle and INP populations. We achieved closure in some circumstances within uncertainties, but we emphasize the need for freezing parameterization of potentially missing INP types and evaluation of the choice of parameterization to be employed. Overall, this closure pilot study aims to assess the level of parameter details and measurement strategies needed to achieve aerosol–ice formation closure. The closure approach is designed to accurately guide immersion freezing schemes in models, and ultimately identify the leading causes for climate model bias in INP predictions.

**KEYWORDS:** Aerosols; Cloud microphysics; Glaciation; Aerosol indirect effect; Aerosol-cloud interaction; Aerosols/particulates

<https://doi.org/10.1175/BAMS-D-20-0151.1>

Corresponding author: D. A. Knopf, [daniel.knopf@stonybrook.edu](mailto:daniel.knopf@stonybrook.edu)

Supplemental material: <https://doi.org/10.1175/BAMS-D-20-0151.2>

In final form 19 May 2021

©2021 American Meteorological Society

For information regarding reuse of this content and general copyright information, consult the [AMS Copyright Policy](#).

**AFFILIATIONS:** Knopf, Li, Lu, and Wang—Stony Brook University, State University of New York, Stony Brook, New York; Barry, Moore, Levin, Creamean, Hill, and DeMott—Colorado State University, Fort Collins, Colorado; Brubaker, Jahl, Monroe, and Sullivan—Carnegie Mellon University, Pittsburgh, Pennsylvania; Jankowski, Rivera-Adorno, Tomlin, and Laskin—Purdue University, West Lafayette, Indiana; Saucedo, Vepuri, and Hiranuma—West Texas A&M University, Canyon, Texas; Shi and Liu—Texas A&M University, College Station, Texas; Lata and China—Environmental Molecular Sciences Laboratory, Pacific Northwest National Laboratory, Richland, Washington; Alpert—Laboratory of Environmental Chemistry, Paul Scherrer Institute, Villigen, Switzerland; Moffet—Sonoma Technology, Inc., Petaluma, California; Fridlind—NASA Goddard Institute for Space Studies, New York, New York; West and Riemer—University of Illinois at Urbana–Champaign, Urbana, Illinois

**A**ccurate prediction of ice crystal formation from aerosol particles acting as ice-nucleating particles (INPs) in cloud and climate models represents a grand challenge (Boucher et al. 2013). This difficulty arises because there are several ice nucleation pathways leading to primary ice crystal formation (Pruppacher and Klett 1997; Vali et al. 2015). Also, aerosol particles exhibit a wide range of physicochemical particle properties such as size, composition, and morphology, all of which impact the particle's ice nucleation activity (Cziczo et al. 2017; Hoose and Möhler 2012; Kanji et al. 2017; Knopf et al. 2018; Murray et al. 2012). Although relatively weak supersaturations are required to activate a majority of sufficiently large aerosol particles as cloud condensation nuclei (CCN), only a small fraction will be activated as INPs (DeMott et al. 2010; DeMott et al. 2011).

The last 20 years have seen a surge of laboratory, field, and instrument intercomparison studies of ice nucleation, advancing the analytical techniques and the understanding of the underlying processes that yield INPs (Burkert-Kohn et al. 2017; DeMott et al. 2015, 2017, 2011, 2018; Hiranuma et al. 2015, 2019; Kanji et al. 2017; Knopf et al. 2018). Ultimately, the acquired ice nucleation data for various inorganic, organic, and biological INP types combined with the knowledge of the ambient aerosol particle size distribution (PSD) and its composition should allow prediction of the INP number concentration for a given environmental temperature and humidity. To robustly evaluate our predictive capability of ice formation by immersion freezing in natural environments, we turned to a closure approach, which has been widely used to similarly test models for aerosol optical properties and CCN activation (e.g., Quinn and Coffman 1998; VanReken et al. 2003). Owing to the considerable challenge of adequately characterizing an aerosol population sufficiently to predict the fraction acting as INPs, we conducted a pilot study at the U.S. DOE Atmospheric Radiation Measurement (ARM) user facility at Southern Great Plains (SGP) during October 2019 to test a field observational approach for achieving aerosol–ice formation closure, termed Aerosol–Ice Formation Closure Pilot Study (AEROICESTUDY). For this pilot study, we focus solely on immersion freezing at water saturation, which is thought to be the dominant primary ice formation process in mixed-phase clouds (Ansmann et al. 2009; de Boer et al. 2011; Westbrook and Illingworth 2013), and can also play a role in cirrus cloud formation (Haag et al. 2003; Heymsfield et al. 1998; Seifert et al. 2004). In climate models, changes in extratropical cloud phase (more liquid versus ice) have been tied to higher equilibrium climate sensitivity (Tan et al. 2016; Zelinka et al. 2020), and process studies show how the liquid phase is modulated by ice formation under typical mixed-phase conditions (e.g., Ovchinnikov et al. 2014), motivating assessment of immersion INP schemes.

The main objective and research questions which guided the design of this closure study are summarized in Table 1. The overall objective of AEROICESTUDY is to evaluate the necessary observations required to achieve closure, and thus robustly assess immersion

freezing parameterizations that are best suited for implementation in cloud and climate models. Figure 1 exemplifies the challenges climate models face in representing INP number concentrations (Fig. ES1 in the online supplemental material displays the closure case study on 15 October; <https://doi.org/10.1175/BAMS-D-20-0151.2>). The Community Atmospheric Model, version 6 (CAM6; supplemental material), reproduces the meteorological conditions well at the location of the field campaign when nudged toward the Modern-Era Retrospective Analysis for Research and Applications, version 2 (MERRA-2), meteorology reanalysis (Gelaro et al. 2017). However, mass concentrations of PM<sub>2.5</sub> and fine mineral dust (both for particulate matter < 2.5 μm in diameter) are underestimated compared to long-term observations from a nearby Interagency Monitoring of Protected Visual Environments (IMPROVE) site. Last, the predicted INP number concentrations at -20°C and their temporal trends over the campaign period, using two different immersion freezing parameterizations, do not follow the observed INP number concentrations during AEROICESTUDY, emphasizing the importance of an improved representation of INPs. Our closure exercise, below, indicates that the underestimation of the fine mineral

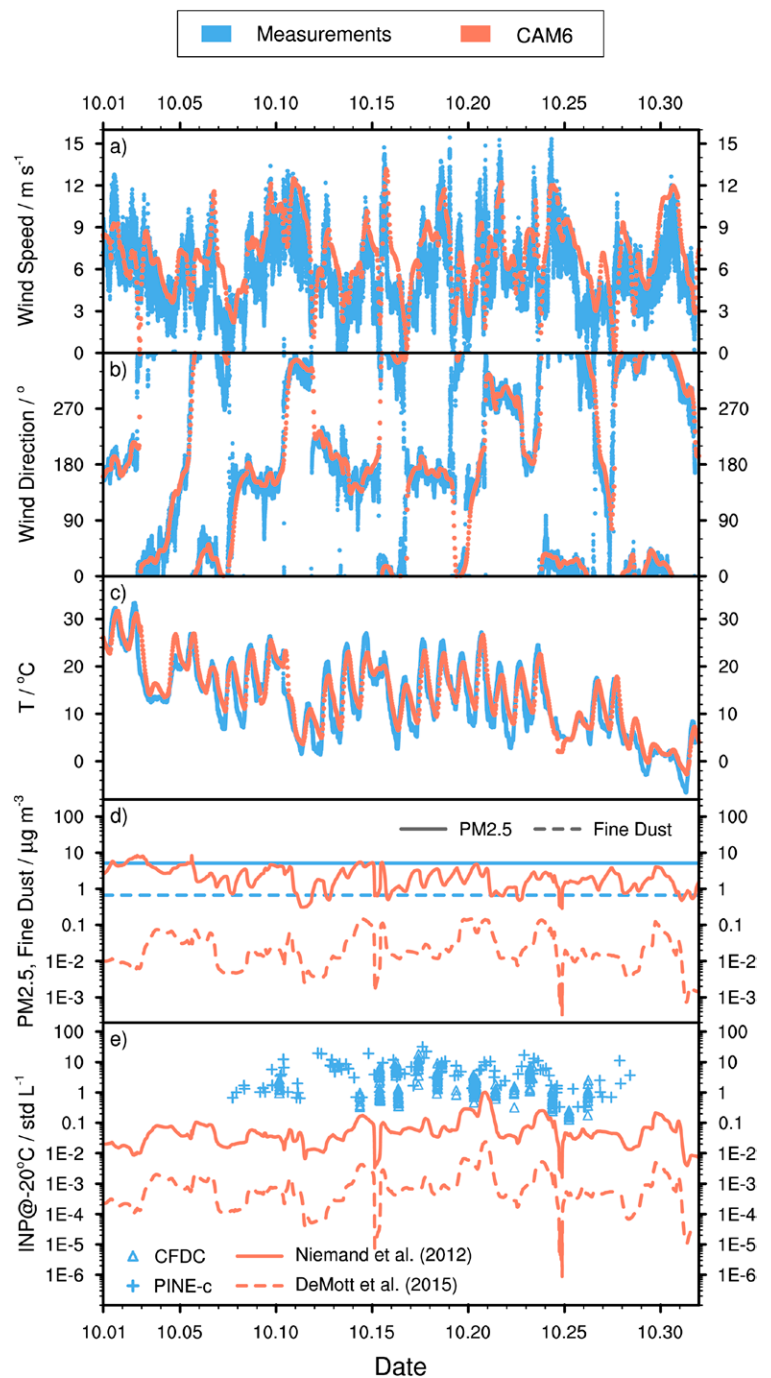


**Fig. 1.** Time series of Community Atmospheric Model, version 6 (CAM6), simulated (orange) and measured (blue) (a) wind speed, (b) wind direction, (c) temperature, (d) particulate matter with a diameter smaller than 2.5 μm (PM<sub>2.5</sub>, thick lines) and dust load (thin lines), and (e) ice-nucleating particles (INPs) at -20°C during the entire field campaign. Meteorology data in (a)–(c) were obtained from DOE ARM SGP E13 station. Blue lines in (d) are the median value of Interagency Monitoring of Protected Visual Environments (IMPROVE) observation in October from 2002 to 2009 at Cherokee Nation, Oklahoma (CHER1). The thick orange line in (e) represents the parameterization by Niemand et al. (2012), and the thin orange line represents the parameterization by DeMott et al. (2015). Blue triangles and pluses are INP measurements by Continuous Flow Diffusion Chamber (CFDC) and Portable Ice Nucleation Experiment (PINE-c), respectively.

**Table 1. Objective and research questions that guided the Aerosol–Ice Formation Closure Pilot Study.**

Overall objective	Identify ice nucleation parameterizations that produce the most robust predictions of INP number concentrations and thus are best suited to be included in cloud and climate models.
Research question 1	What are the crucial aerosol physico-chemical property measurements needed to accurately guide ice nucleation representations in models and long-term INP measurements?
Research question 2	What level of parameter details needs to be known to achieve aerosol–INP closure?
Research question 3	What are the leading causes for climate model bias in INP predictions?

dust concentrations is at least one reason for model underestimation of INP number concentrations. Here, we demonstrate the closure concept via an initial investigation of data collected on one day out of the full campaign period. While time series of a subset of the collected data streams are presented for the entire campaign, we focus on the initial analysis of a single day to demonstrate the principles of an aerosol–ice formation closure study. This is because automated but also manual analyses of large single particle datasets are needed for drawing statistically robust conclusions as well as investigating short-term variability. Nevertheless, data and physical samples remain for substantive analysis in the future.

For this case study we apply the INP parameterization by DeMott et al. (2010, 2015), the ice nucleation active sites (INAS) approach (Connolly et al. 2009; DeMott 1990) both based on the singular hypothesis, and the water activity-based immersion freezing model (ABIFM) (Alpert and Knopf 2016; Knopf and Alpert 2013) based on classical nucleation theory (CNT) accounting for time and stochasticity of nucleation. Each of these parameterizations requires different information about the aerosol particle population as inputs, which is discussed in detail below. Hence, for this closure exercise, adequate characterization of the aerosol population is as critical as the measurement of INP number concentrations. Since immersion freezing scales with INP surface area (e.g., Beydoun et al. 2016; Kanji et al. 2008; Knopf et al. 2018), this study includes the characterization of the supermicron-sized aerosol population, which can at times dominate total aerosol surface area.

**Closure concept.** Figure 2 displays the concept of AEROICESTUDY: we measure all model inputs as well as predicted outputs, and then evaluate whether the model can predict the measured outputs when measurement uncertainties are accounted for. To achieve this, the aerosol population is concurrently sampled by online and offline physical, chemical, and INP instrumentation (Table A1 in the appendix). The measured particle properties are merged (i.e., with respect to size and composition) to serve as representative input for the applied immersion freezing parameterizations. The predicted INP number concentrations are then compared to measured INP number concentrations after accounting for particle transmission losses in instrumentation inlets and uncertainties in measurements and parameterization. An agreement between measured and predicted INP number concentrations within determined uncertainties indicates successful closure. Owing to the relatively demanding nature of the input data required, conducting the pilot study at a ground site offers the benefits of relatively elevated INP concentrations (thereby improving signal to noise) and relatively less expensive

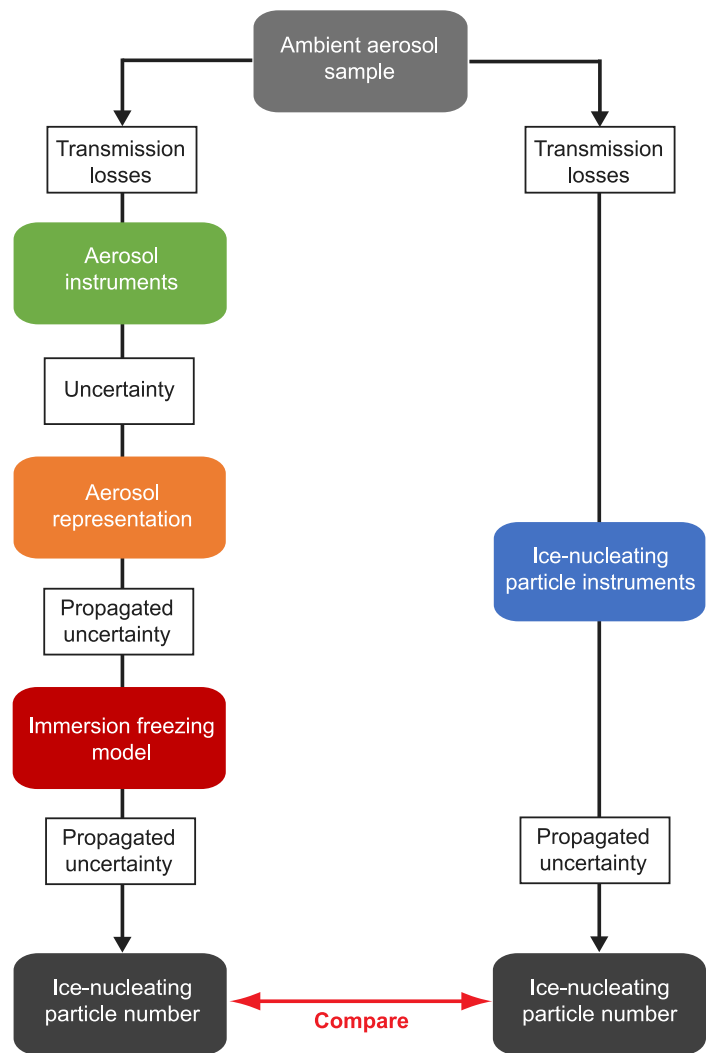


Fig. 2. Schematic showing the conceptual approach of the aerosol–ice formation closure pilot study.

operations (allowing many hours of deployment). Results of ongoing analyses will help clarify the feasibility for aircraft deployment (e.g., sampling time and detection limit requirements across the instrument array).

### Sampling site and methods

Most online and offline instrumentation was located in the Guest Instrument Facility (GIF) at SGP, in Oklahoma, in a rural setting, dominated by agricultural activities including cattle pasture and wheat fields. Particles were sampled from the base of a custom-built high-volume sampling stack, 6 in. in diameter and reaching about 1.5 m above the GIF roof line (Fig. 3). Blowers at the end of the stack produced a downward airflow of about  $1 \text{ m s}^{-1}$ . The instrumentation sampled from the center of the stack, with respective isokinetic sampling tubes and varied pumping speeds (Table A1), resulted in a range of slightly sub- to superisokinetic sampling. Size-resolved particle transmission losses in sampling tubes routed to the instrument inlets were estimated using a particle loss calculator (von der Weiden et al. 2009). Some additional offline measurements were made, positioned close to the stack intake (Fig. 3). An aerosol concentrator (supplemental material) was also placed on the platform, using a smaller line into the GIF, with minimal bends, to feed two online instruments.

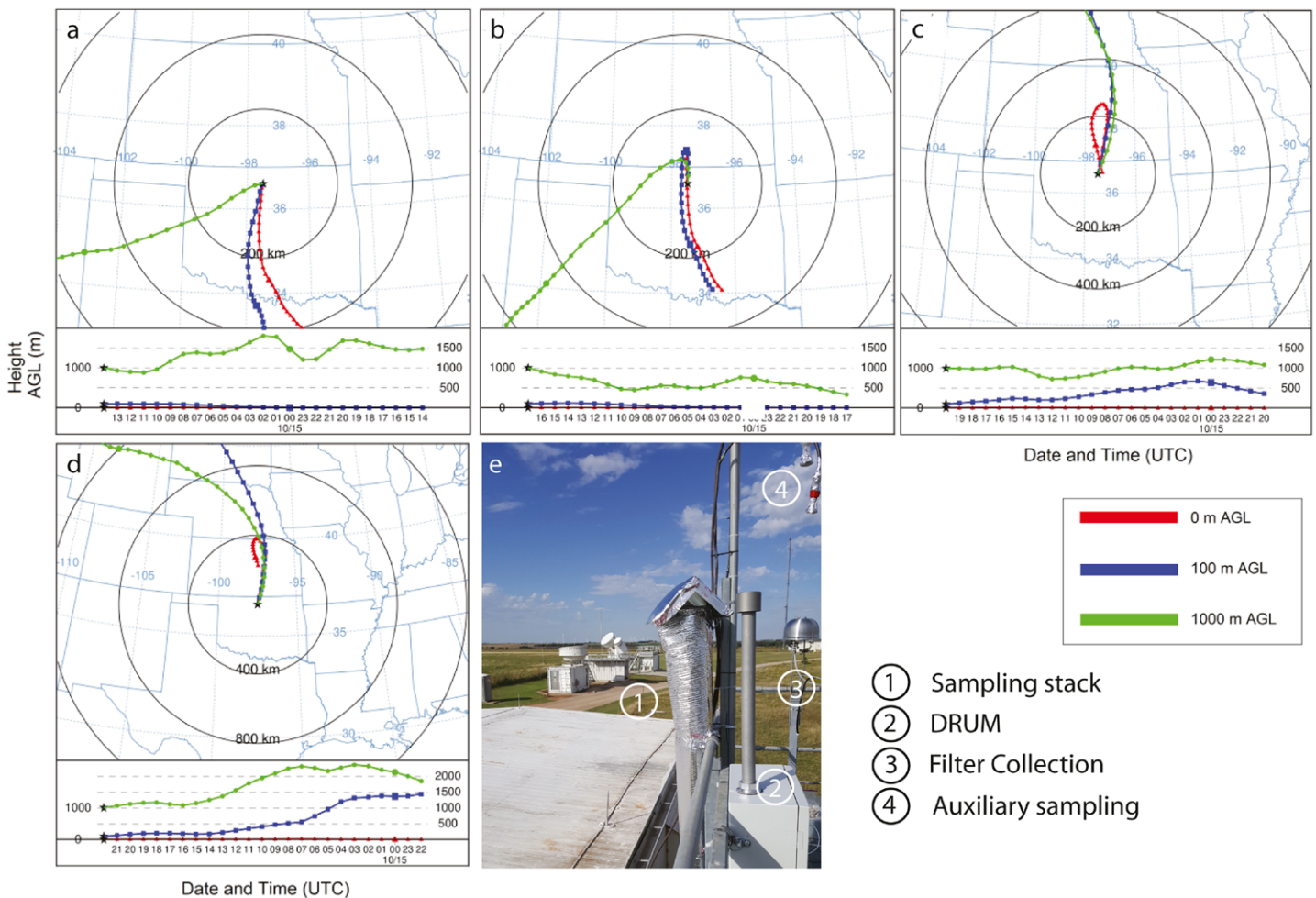


Fig. 3. The AEROICESTUDY was conducted at the U.S. DOE Atmospheric Radiation Measurement (ARM) user facility at the Southern Great Plains (SGP;  $36.605438^{\circ}\text{N}$ ,  $97.485788^{\circ}\text{W}$ ) Central Facility using the Guest Instrument Facility (GIF). NOAA HYSPLIT 24-h backward trajectory calculations are given for the frontal passage event at (a) 0900, (b) 1200, (c) 1500, and (d) 1700 CDT 15 Oct for 0, 100, and 1,000 m above ground level (AGL). (e) A high-volume sampling stack was mounted to the GIF observation platform which also housed Davis Rotating-drum Unit for Monitoring (DRUM), filter collection, and auxiliary sampling inlets.

## Measurements

Table A1 provides an overview of the online and offline instrumentation employed in this closure study, including brief information on the particle size range, sample amount, and sampling frequency. The supplemental material gives a short description of each employed instrument system and references. As outlined below, the various instrument sampling conditions must be accounted for in the quantitative closure.

For this closure exercise we concurrently measured particle properties and INP number concentrations for defined time periods. This entailed a morning period, typically, from about 0900 to 1200 LT and an afternoon period usually from 1300 to 1700 LT. However, those time periods were adjusted accordingly to capture interesting events in aerosol PSD or composition and meteorology. Some of the online instrumentation allowed for almost continuous sampling over the entire campaign period. Aerosol PSDs were measured using a scanning mobility particle sizer spectrometer (SMPS) and aerodynamic particle sizer spectrometer (APS) from the stack. To merge SMPS data (electrical mobility diameter) with APS data (aerodynamic diameter), we derived the size distribution correction factor (Khlystov et al. 2004) using SMPS and APS data from the permanent instruments at ARM SGP for the same time periods sampled nearby (supplemental material). This factor was applied to the APS instrument operated by the AEROICESTUDY and resulted in a unified PSD at time intervals of 4 min. A summary of the measured PSD is given in Fig. 4a, reflecting for the most part typical continental PSDs. During the campaign, submicron particle numbers were between 2,000 and 4,000  $\text{cm}^{-3}$  with some days having greater particle concentrations and daily variability. Supermicron particle numbers were typically between 2 and 5  $\text{cm}^{-3}$  with 4 days having higher concentrations.

The focus of the online INP measurements was to probe immersion freezing at a temperature range between  $-20^{\circ}$  and  $-30^{\circ}\text{C}$  at saturated and supersaturated conditions. Figure 4a depicts the INP number concentrations measured by the Portable Ice Nucleation Experiment chamber (PINE-c) and the Continuous Flow Diffusion Chamber (CFDC) for the entire campaign period, demonstrating reliable instrumentation performances. Figure ES2 provides an enlarged view of Fig. 4a for the closure case study on 15 October. As outlined in the supplemental material, the instruments sample different upper size bounds of the ambient particle population (5- and  $2.5\text{-}\mu\text{m}$  aerodynamic diameter for PINE-c and CFDC, respectively) and employ different approaches to induce immersion freezing (i.e., an expansion chamber versus a diffusion chamber). As such, the time resolution and variation of probed freezing temperatures differ between the instruments. During the campaign, the PINE-c operated continuously and the CFDC was operated only during targeted closure exercise periods. Both instruments detected between 1 and 100  $\text{INP L}^{-1}$  for freezing temperatures between  $-20^{\circ}$  and  $-30^{\circ}\text{C}$  with occasional instances where INP number concentrations exceeded  $100 \text{ L}^{-1}$ .

Figure 4a provides an indication of the role of supermicron-sized particles acting as INPs. Over the campaign, several instances occurred when increased supermicron number concentrations correlated with increased INP number concentrations, e.g., during the afternoons on 15, 17, and 21 October. In contrast, supermicron-sized particle number concentrations were lower on 11 October, and on the mornings of 14, 15, and 25 October, they correlated with lower INP number concentrations. Figure 4b displays offline INP number concentration measurements for the closure case study on 15 October (see supplemental material for instrument details). Three offline methods, the Ice Spectrometer (IS), Microfluidic Ice Nucleation Technique (MINT), and Multi Orifice Uniform Deposition Impaction–Droplet Freezing Technique (MOUDI-DFT) provide INP number concentrations for the morning and afternoon periods from aerosol substrate samples indicating about  $1\text{--}1,000 \text{ INP L}^{-1}$  in the temperature range from  $-20$  to  $-30^{\circ}\text{C}$ . The Davis Rotating-drum Unit for Monitoring (DRUM) collected particles, in a

size-segregated manner, for 24 h. DRUM coupled with a Cold Plate (DRUM-CP) for size-resolved bulk immersion freezing demonstrates that INP number concentrations increase when applying samples that contain larger particles where the sample with the largest particles (5–12  $\mu\text{m}$ ) displays from about 0.6 to  $>10$  INP  $\text{L}^{-1}$  for the temperature range from  $-20^\circ$  to  $-27^\circ\text{C}$ .

### Closure case study

We discuss the 15 October closure case in more detail as an example. This campaign date represents an interesting scenario due to the contrasting meteorological conditions and aerosol populations during the morning and afternoon, before and after a frontal passage. We perform closure calculations using online INP instrumentation, PINE-c and CFDC, for morning (0800–1030 LT) and afternoon (1400–1800 LT) hours.

**Meteorology.** On 15 October a cold front passed through the region of the campaign site. Figure 3 shows air parcel backward trajectories calculated using the Hybrid Single-Particle Lagrangian Integrated Trajectory model (HYSPLIT) (Stein et al. 2015) indicating the change in wind direction from the south during the morning and shifting to the north around noon. This was accompanied by a decrease in relative humidity (RH) and increase of wind speed from morning to afternoon hours (Fig. ES3). Aerosol populations varied across this transition, allowing evaluation of our predictive capability of immersion freezing.

**Aerosol population characteristics.** The mean PSDs show a clear distinction between morning and afternoon (Fig. ES4). During the morning, submicron-sized particle number

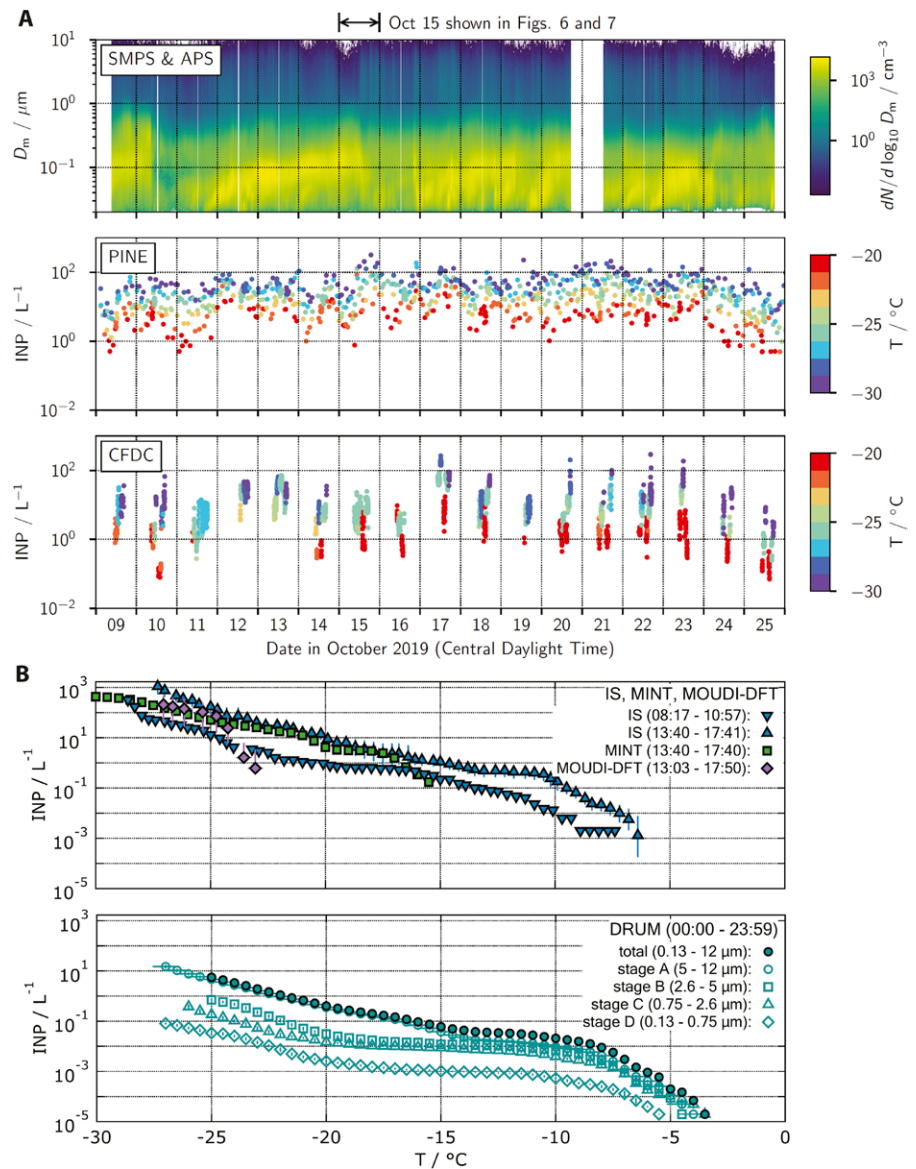


**Fig. 4.** Overview of online measurements (a) for entire campaign period and (b) for offline INP measurements for presented closure case on 15 Oct. Panel (a) shows particle size distributions from combined measurements by scanning mobility particle sizer (SMPS) spectrometer and aerodynamic particle sizer (APS) spectrometer and INP number concentrations with associated freezing temperatures measured by PINE-c and CFDC. INP measurements were done for specific daily time periods and defined temperatures for closure exercises. Panel (b) shows INP number concentrations measured by Ice Spectrometer (IS) for morning and afternoon, Microfluidic Ice Nucleation Technique (MINT) and Multi Orifice Uniform Deposition Impaction Droplet Freezing Technique (MOUDI-DFT) for the afternoon and DRUM for size-resolved INP number concentrations for a 24-h period.

concentrations were enhanced compared to the afternoon while during the drier and windier afternoon, supermicron particle number concentrations were elevated. An overview of the aerosol composition derived by online and offline instrumentation is given in Fig. 5. Figures 5a and 5b summarize the online measurements made by the Laser Ablation Aerosol Particle Time-of-Flight Mass Spectrometer (LAAPTOF) and Soot-Particle Aerosol Mass Spectrometer (SP-AMS), respectively. LAAPTOF, analyzing particles up to  $3\ \mu\text{m}$  in aerodynamic diameter, indicated that mixed, aged inorganic–organic carbon particles dominated the ambient particle population in the morning with decreasing numbers toward afternoon while mineral-organic particle numbers displayed an increasing trend. The SP-AMS showed that, during the morning, the submicron aerosol population was dominated by aged/oxidized organic particles with decreasing concentrations in the afternoon. Both online aerosol composition measurements suggest the presence of aerosol particles that were highly aged, secondary in nature, and mixed. Online measurement with the Wideband Integrated Bioaerosol Sensor (WIBS) corroborate increases in total supermicron particle number concentrations and indicate increases also in fluorescent biological aerosol particle (FBAP) number concentrations by about 3–4 times during the afternoon (Fig. ES5).

Particle-type composition and mixing state of individual particles collected by MOUDI on substrates were also examined by chemical imaging methods, including computer-controlled scanning electron microscopy with energy dispersive X-ray analysis (CCSEM/EDX) and

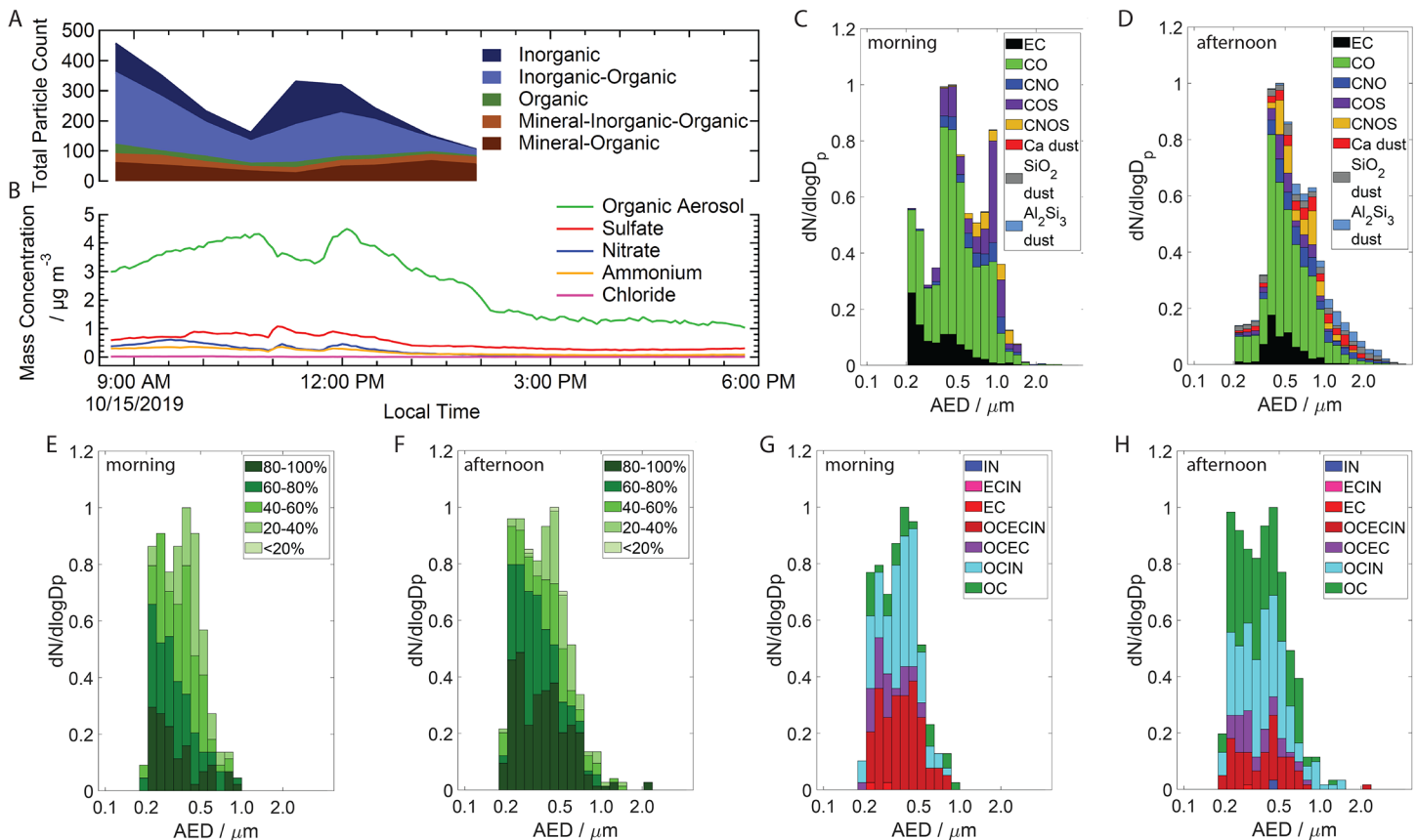


**Fig. 5.** Ambient particle composition for frontal passage closure case study on 15 Oct determined by online and offline instrumentation. (a),(b) Time evolution of particle mixing state and composition analysis by Laser Ablation Aerosol Particle Time-of-Flight Mass Spectrometer (LAAPTOF) and of nonrefractory submicrometer aerosol composition derived by aerosol mass spectrometer (SP-AMS), respectively. (c)–(h) Size-resolved [in area equivalent diameter (AED)] single-particle microspectroscopic analyses. Computer-controlled scanning electron microscopy with energy dispersive X-ray analysis [CCSEM/EDX; (c) and (d)] provide elemental particle composition where EC: elemental carbon; CO: carbon, oxygen; CNO: carbon, nitrogen, oxygen; COS: carbon, oxygen, sulfate; CNOS: carbon, nitrogen, oxygen, sulfate. Scanning transmission X-ray microscopy with near-edge X-ray absorption fine structure spectroscopy [STXM/NEXAFS; (e)–(h)] providing organic volume fraction (OVF) per particle [(e) and (f)] and particle mixing state [(g) and (h)] where IN: inorganic; EC: elemental carbon; OC: organic carbon.



scanning transmission X-ray microscopy with near-edge X-ray absorption fine structure spectroscopy (STXM/NEXAFS). In addition, particle samples were used in offline immersion freezing experiments by MOUDI-DFT. The samples applied for this closure case study are described in Table ES1.

CCSEM/EDX was employed to determine the size-resolved particle-type distribution in the ambient aerosol population using *k*-means cluster analysis (e.g., Knopf et al. 2014) displayed in Figs. 5c and 5d (Figs. ES6a and ES6d show the fractional size-resolved particle-type distribution). This method allows the identification of major particle types within the population with high significant representativeness due to the large number of particles being analyzed (Thompson 1987; Wang et al. 2012a). The composition of the identified major particle types is displayed in Fig. ES7. This analysis shows the dominance of carbonaceous organic (CO), inorganic–organic (CNO, COS, CNOS), and soot [elemental carbon (EC)] particle types during the morning (Fig. 5c). In contrast, in the afternoon, larger particles were present and the fraction of mineral particle types (e.g., Ca, SiO<sub>2</sub>, and Al<sub>2</sub>Si<sub>3</sub> dust) was greater. Figure ES8 illustrates typical electron microscopy (EM) images of particles collected during the morning and afternoon corroborating the different nature of the major particle types. The CCSEM/EDX derived characterization of the ambient particle populations serves to initiate the particle population composition for the closure exercise.

We performed STXM/NEXAFS to infer the size-resolved particle mixing state of the aerosol population (Figs. 5e–h) with the fractional distribution given in Figs. ES6b, ES6c, ES6e, and ES6f. STXM/NEXAFS was performed at the carbon K-edge, thus allowing chemical speciation of the organic carbon (OC) particles (Hopkins et al. 2007; Knopf et al. 2014; Moffet et al. 2010a,b). EC is identified by the carbon double bond and oxygenated OC by the presence of carboxyl groups. Figures 5e and 5f display the organic volume fraction (OVF) for the morning and afternoon particle population. The analysis demonstrates that all particles in these two populations were associated with organics. The afternoon showed a larger number of particles dominated by organics, even at the largest examined sizes, and the presence, albeit minor, of particles with OVF < 20% indicating the appearance of inorganic (IN) species, likely of mineral dust. This is corroborated by the compositional maps shown in Fig. ES9. The afternoon particle population can be clearly distinguished from the morning in having larger organic-dominated particles. The corresponding population mixing state analysis further supports this trend as shown in Figs. 5g and 5h. In the morning inorganic–organic particles dominate the population (OCIN, OCECIN) whereas in the afternoon a greater number of all particles and larger particles are pure organic and inorganic–organic in nature. Less elemental carbon was also present.

Realizing the importance of supermicron particles for immersion freezing (Fig. 4), we analyzed this larger particle-type class (up to 6 μm) by SEM/EDX. Since particle concentrations in this size range were low (Fig. 4 and Fig. ES4), particle loading on substrates was also low, making it difficult to generate statistically significant particle population information (compared to the case above). Thus, these analyses are limited to assisting interpretation of our closure calculations below. Figures ES10a and ES10b show that the supermicron particle types in the morning are mostly inorganic (nonmineral) and organic with some mineral dust, whereas mineral dust and biological particle-type numbers were greater in the afternoon. The latter result is consistent with the WIBS results. Figure ES10c provides typical atomic composition and electron microscopy images of these identified particle types.

**Aerosol–INP closure calculations.** The established physicochemical properties of the ambient aerosol population serve as input parameters to predict the INP number concentration by immersion freezing for the selected time periods and conditions produced by the PINE-c and

CFDC. The applied sampling inlets resulted in minor particle losses (see also supplemental material). Thus, online instrumentation sampled the same PSD, except for the differences in the upper size cutoff, and particle losses do not have a significant impact on the closure calculations.

**PARTICLE COMPOSITION.** The CCSEM/EDX derived morning and afternoon representative particle type populations (Fig. 5) were merged with the PSD to allow for the particle-type speciation of aerosol entering the online INP instrumentation. The closure calculation accounts for the different PSD sampled by the two INP instruments. We apply the derived particle-type population for the entire morning and afternoon measurement period (Fig. 5). However, this particle-type population had to be further simplified to allow application of commonly used immersion freezing parameterizations and to assess the necessary level of detail for implementing INP prediction in cloud and climate models.

**IMMERSION FREEZING PARAMETERIZATION.** The INP parameterizations of DeMott et al. (2010, 2015) are designed to be applied to atmospheric particles in general and mineral dust specifically, respectively, and require the number concentration for particles (total and mineral dust only, respectively) larger than  $0.5\text{-}\mu\text{m}$  diameter and freezing temperature as input. The upper size limit of the data for derivation of the INP parameterization of DeMott et al. (2010) was limited to  $\sim 1.6\ \mu\text{m}$ . Hence application to larger-sized particles may result in a prediction bias as discussed in DeMott et al. (2010). Similarly, the INP parameterization by DeMott et al. (2015) is based on employed dust PSDs. Significant differences to those, that might be possible at this ground sampling site, may impact predictions of INP number concentrations. Application of INAS and ABIFM parameterizations require, in addition, the INP type and its surface area (see also supplemental material). The INAS reports the temperature-dependent freezing capability of an INP in terms of an ice nucleation active site density,  $n_s(T)$  (in  $\text{m}^{-2}$ ) (Connolly et al. 2009). ABIFM reports the heterogeneous ice nucleation rate coefficient,  $J_{\text{het}}(T)$ , (in  $\text{m}^{-2}\ \text{s}^{-1}$ ) (Knopf and Alpert 2013). Predicted INP number concentrations are then derived by multiplying INP-type surface area with the corresponding  $n_s(T)$  and  $J_{\text{het}}(T)$  values, where in the latter case a nucleation time is required. Since INAS and ABIFM immersion freezing parameterizations are not available for each identified particle type, we grouped observed particle types into well-studied INP types; this procedure constitutes another necessary simplification. In this first closure attempt we applied three INP types: soot, organic, and mineral dust. This assumes that these INP types represent particles at SGP adequately. For soot INPs we use the recently published INAS parameterization by Schill et al. (2020), which is also used to derive an ABIFM parameterization (supplemental material and Fig. ES13). However, it is not expected that soot particles impact total INP number concentrations significantly in the immersion freezing regime (Kanji et al. 2020; Schill et al. 2020).

For application in INAS and ABIFM we use the immersion freezing parameterization for organics (represented by a humic acid compound) derived by China et al. (2017), Knopf and Alpert (2013), and Rigg et al. (2013). We apply the INAS desert dust (DD) parameterization by Niemand et al. (2012) and its ABIFM derivation (Alpert and Knopf 2016) representing mineral dust. Each parameterization is associated with uncertainties and those are applied as reported in the literature (view supplemental material and Table ES2). It is important to note that uncertainty for each parameterization was not calculated the same way and may differ based on what metric was used, e.g., data scatter, standard deviation, confidence and prediction band intervals, or fiducial limits. Therefore, the uncertainties propagated to INP number concentrations do not indicate whether or not one parameterization is more or less certain than the other. Figure ES14 displays the applied size-resolved particle-type population

to predict INP number concentrations for the morning and afternoon. The fraction of particles containing EC were combined to represent soot particles, all particles containing organics (including inorganic–organic particle types) were lumped together as organics (org), and all identified mineral-type classes (Fig. ES7) were expressed as mineral DD (Figs. 5c and 5d). The effective measurement size range for CCSEM/EDX is from approximately 350 nm to 3  $\mu\text{m}$ . Below 350 nm, we assumed a composition equal to the average composition between 350 and 500 nm (supplemental material). As such, the morning is dominated by organic and soot particles whereas the afternoon is dominated by mineral dust and organic particles. Another caveat, not treated in this first closure exercise, is related to the presence of inorganic and/or organic coatings of soot and mineral dust and its unresolved (i.e., enhancing or diminishing) impact on immersion freezing (Augustin-Bauditz et al. 2016; Kanji et al. 2019; Knopf et al. 2018; Möhler et al. 2008; O’Sullivan et al. 2016; Sullivan et al. 2010). Furthermore, we likely overestimate the INP surface area of organic and organic-coated particles since some of these organic compounds might deliquesce under immersion freezing conditions (Berkemeier et al. 2014; Charnawskas et al. 2017; Knopf et al. 2018; Wang et al. 2012b).

ABIFM requires an instrument characteristic nucleation time. For PINE-c, the INP number concentrations were determined at the lowest reported 2°C temperature interval (reflecting the  $\pm 1^\circ\text{C}$  uncertainty). Typically, the total temperature decrease in individual expansions is  $4.7^\circ \pm 2.1^\circ\text{C}$ . Depending on the lowest temperature of the expansion the nucleation time varies between about 13 and 48 s (supplemental material). For the CFDC, the residence times of the aerosol particles in the chamber at supersaturation provides the nucleation time, which is 5 s (DeMott et al. 2015).

**CLOSURE CALCULATIONS FOR PINE-C DATA.** Figure 6 displays the closure calculations for PINE-c-derived INP number concentrations. Uncertainty derivation of predicted INP number concentrations is outlined in the supplemental material and Table ES2. Observed INP number concentrations ranged from around  $1 \text{ L}^{-1}$  at  $-20^\circ\text{C}$  to  $100 \text{ L}^{-1}$  at  $-28^\circ\text{C}$ . The parameterization by DeMott et al. (2010) captures measured INP number concentrations within experimental and model uncertainty, whereas DeMott et al. (2015) significantly underpredicts observed INP number concentrations. This is expected since the DeMott et al. (2015) parameterization only considers mineral dust INPs, whereas the morning was dominated by soot and organic particles. Assuming all particles larger than  $0.5 \mu\text{m}$  are treated as mineral dust INPs (DeMott et al. 2015), the predicted INP number concentrations were within the range of INP number concentrations derived from DeMott et al. (2010) and in agreement with observations. This result could hint that some of the organic particles are soil organics which can have similar ice nucleation activity as DD (Tobo et al. 2014).

For INAS application, we consider soot, organic, and DD as INP types. DD contributes significantly to the observed INP number concentrations during the morning (though not much dust is present, Fig. ES14), while organic INPs generate INP number concentrations similar to observed values, but only for the lowest temperature ( $-28^\circ\text{C}$ ). Only in a few instances soot INPs contribute more than organic INPs but were still insufficient to reproduce observed INP number concentrations. The overall predicted INP number concentrations via the INAS method (blue line) underestimated INP number concentrations but captured most measurements within the uncertainty. Assigning all particles as dust INPs greatly overpredicts INP number concentrations. Last, ABIFM shows overall similar INP number concentration trends as INAS and captured most observations within uncertainties. Though organics and soot contribute relatively more to INP number concentrations compared to INAS (recall that organics and soot dominate the morning population). Only for the lowest examined temperature did the organic INPs produce calculated INP number concentration in a similar range to the observations. Again, when all particles are treated as dust INPs, INP number concentrations were overpredicted.

### OTHER POTENTIAL INP TYPES.

The underestimation of INP number concentrations by INAS and ABIFM could be due to the lower ice nucleation activity of the organic INP parameterization applied. If some of the organic particles are secondary or aged in nature, e.g., secondary organic aerosol (SOA), this would impact predicted INP number concentrations. SOA INPs are little studied with varying immersion freezing ability depending strongly on composition and temperature (e.g., Knopf et al. 2018). Anthropogenic SOA from naphthalene precursor gases might exhibit slightly enhanced immersion freezing capabilities compared to applied organic INP (Wang and Knopf 2011; Wang et al. 2012b), though this requires further investigation. The detected inorganic–organic particles could be carbonaceous and organosulfate and organonitrate containing particles (Fig. 5) and representative of biogenic SOA (Wolf et al. 2020). Those particle types were not included in the closure calculations and immersion freezing parameterizations are not available. Organosulfate particles have been shown to act as INPs, however, for lower temperatures than those probed in the current study (Wolf et al. 2020). The organic INP shows similar immersion freezing activity as illite dust (China et al. 2017; Knopf and Alpert 2013) but lower than DD (Niemand et al. 2012). However, soil-organic INPs can possess high freezing capability, similar to DD, and if some of the organic particles would fall into this class, better agreement between prediction and observation would be achieved. This is corroborated by offline IS measurements (Fig. ES15), where chemical treatments indicate the presence of organic INPs active at  $-20^{\circ}\text{C}$  and lower, and these are not captured by the applied organic INP parameterization.

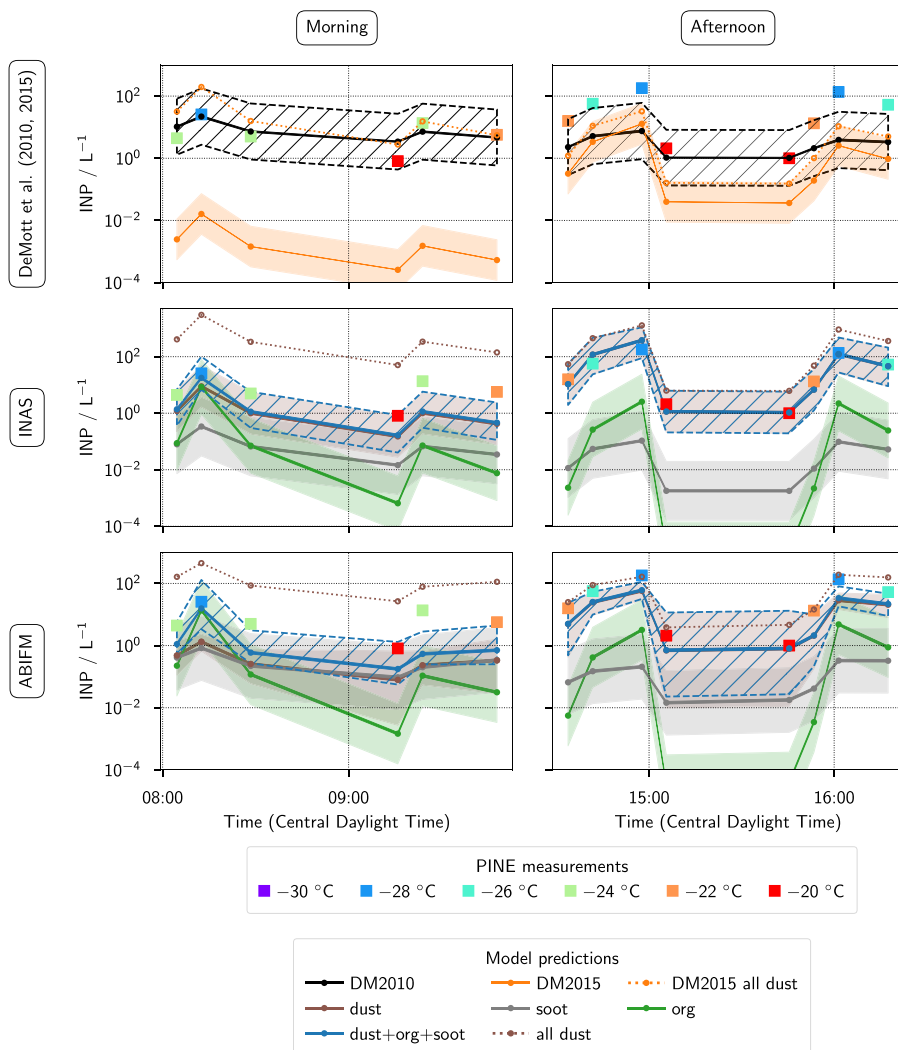


**Fig. 6.** INP number concentrations measured by PINE-c at different freezing temperatures for closure case study on 15 Oct for morning and afternoon periods (large colored squares). Uncertainties in measured INP number concentrations are about  $\pm 20\%$ . Solid lines, small circle symbols, and corresponding shading represent predicted INP number concentrations. (top) INP number concentrations predicted by DeMott et al. (2010, 2015) parameterizations as black and orange lines, respectively. The dotted orange line represents the prediction by the DeMott et al. (2015) parameterization assuming all particles larger than  $0.5\ \mu\text{m}$  are acting as mineral dust INPs. (middle) INP number concentration predictions by the ice nucleation active sites model (INAS) applying parameterizations for organic (green), soot (gray), and mineral dust (brown) INPs (see text for more details). Blue line represents total INP number concentrations from all individual INP types. Dotted brown line displays INP number concentrations when all particles are assumed to be mineral dust particles. (bottom) INP number concentration predictions by the water activity–based immersion freezing model (ABIFM) where lines are the same as for the INAS case in middle panels.

For the afternoon, PINE-c observed INP number concentrations from 1 to 100 L<sup>-1</sup>, where lower temperatures yielded higher INP number concentrations. During the afternoon higher concentrations of mineral dust, organic, and biological particles were present compared to the morning. The DeMott et al. (2010) parameterization underestimated most of the observed INP number concentrations, capturing the observed INP number concentration only at the highest temperatures. Application of the DeMott et al. (2015) parameterization, applicable to mineral dust, yielded similar INP number concentrations as the DeMott et al. (2010) parameterization at lower temperatures, but at higher temperatures predicted lower INP number concentrations than were observed. Assuming all particles are mineral dust increases, INP number concentrations produced and the predicted trends are in agreement with observations within uncertainties, but the predicted values still underestimate observed concentrations.

For the INAS case, DD completely dominates the overall INP number concentrations (the blue line is on top of the brown line) and mostly captured the observations. It also follows the trend of observed INP concentrations under changing freezing temperatures. Predicted soot and organic INPs do not contribute significantly to total INP number concentrations. The INAS DD parameterization represented and slightly overpredicted the INP number concentrations for most cases. It should be noted that the INAS DD parameterization does not include the effects of inorganic and organic coatings of mineral dust particles (recall that no purely inorganic particles were observed, Fig. 5) that might impact the freezing efficiencies. Here, it was assumed that a potential coating material completely dissolves and presents a negligible constituent in the surrounding water, thus, not causing a freezing point depression (Knopf and Alpert 2013). However, it is known that amorphous OM may not readily dissolve over experimental time scales and thus could impact the freezing efficiency (Berkemeier et al. 2014; Charnawskas et al. 2017; Knopf et al. 2018). Furthermore, in light of the WIBS data indicating higher FBAP concentrations, centered in the size range larger than single-particle analyses could resolve compositions in a statistical manner (Fig. ES5), the closure calculation likely misclassifies any biological INPs (not parameterized) as dust INPs. IS, MINT, MOUDI-DFT, and DRUM-CP demonstrate INPs active at even higher temperatures than those targeted in this closure case (Fig. 4b) and show that these were organic and biological in origin (Fig. ES15). Looking at the DRUM-CP measurements (Fig. 4b), for the two largest cutoff sizes (2.6–5 and 5–12 μm) representing some of the largest particles sampled by PINE-c about 0.04–0.5 INP L<sup>-1</sup> at –20°C were detected, which would result in a significant contribution to overall INP number concentration at those higher freezing temperatures and which is unaccounted for in the closure calculations. For the INAS application (middle panel, afternoon), if all particles are assumed to be dust INPs the predicted INP number concentrations are overpredicted but much less so than for the morning case since the afternoon particle population contained a significant amount of dust particles. Since INP number concentrations are close to or overpredicted by INAS DD, this would imply a negligible presence of soil-organic INPs, contrary to offline observations. This raises questions about whether INAS can capture the observations for this case. In short, we might overestimate the contribution of DD to observed INP number concentrations but underestimate the contributions of soil organic and FBAP as INPs.

The ABIFM parameterization of DD captured the observed INP number concentrations (the blue line is on top of the brown line); however, in contrast to the INAS case, INP number concentrations were, for most observations, slightly underestimated. Organic and soot INPs did not significantly contribute to the predicted INP number concentrations. Addition of biological INPs in number concentrations suggested by offline analysis (Fig. ES15) might bring ABIFM INP number concentration predictions into closer agreement with observed INP number concentrations. However, the nature of biological particles is not known, and an immersion freezing parameterization for these particles is currently not available and will be investigated in upcoming analyses. Assuming all particles act as dust INPs would bring some ABIFM INP

number concentration predictions into better agreement with observed INP number concentrations. This would be in line with the role of soil organic INPs (in accord with offline measurements, Fig. ES15) that are not included in this closure calculation and also demonstrates the sensitivity of INP number concentrations to different immersion freezing parameterizations and assumption about size-resolved composition. In general, when missing INP types, applied INP parameterizations should underestimate observed INP number concentrations.

Tables ES3 and ES4 provide the contribution of different INP sizes to the overall INP number concentration as predicted by INAS and ABIFM parameterizations, respectively, for PINE-c closure calculations. During morning INPs  $< 1 \mu\text{m}$  in size dominate, and during afternoon INPs in sizes from  $2.5$  to  $5 \mu\text{m}$  similarly contribute to or even dominate the total INP number concentration. This analysis hints to the effect that the surface area of many small particles can compete with the surface area of a few large particles to initiate freezing. This analysis emphasizes the importance of INP size when attempting closure as also evident from the offline INP measurements shown in Fig. 4b.

**CLOSURE CALCULATIONS FOR CFDC DATA.** Figure 7 displays the closure calculations involving CFDC observed INP number concentrations. For the morning CFDC detected about  $1\text{--}10 \text{ INP L}^{-1}$  at  $-26^\circ\text{C}$  whereas after 0900 LT

the INP number concentrations varied, potentially related to the varying wind speeds (Fig. ES3). For the morning period, the DeMott et al. (2010) parameterization captured the observed INP number concentrations well, whereas after 0900 LT the predicted INP number concentrations were in some instances higher than measured INP number concentrations. In general, INAS DD captured measured INP number concentrations, although dust is not abundant during the morning. ABIFM underestimated INP number concentrations and achieved some agreement with observations after 0900 LT. Contrary to INAS, all INP types contributed similarly where organic INPs dominate after 0900 LT, which reflects the morning particle population.

If some soil-organic INPs were not being represented by the organic INP

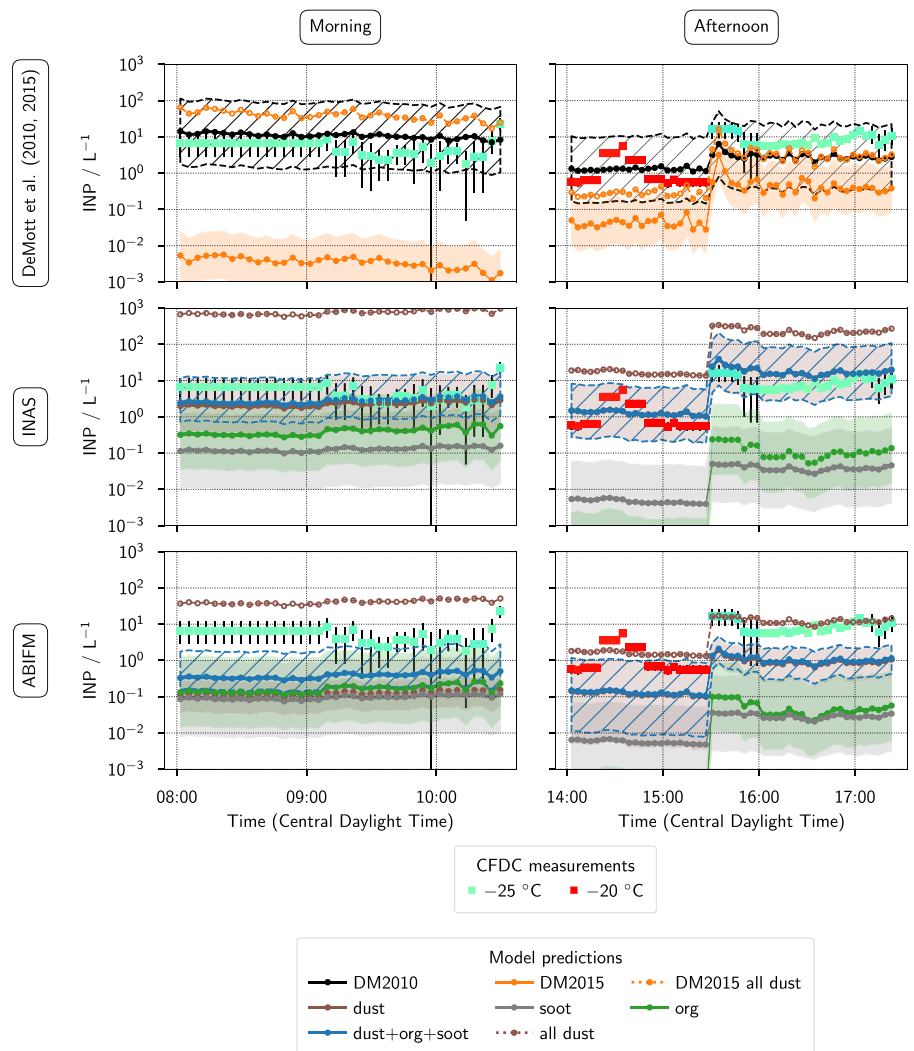


**Fig. 7.** INP number concentrations measured by CFDC for the closure case study on 15 Oct applying different freezing temperatures for morning and afternoon periods (large colored squares). Solid lines, small symbols, and corresponding shading and panels are the same as given in Fig. 6.

parameterization used, as discussed for the closure case in Fig. 6, this could explain the underestimation of INP number concentrations by ABIFM.

During the afternoon, observed INP number concentrations ranged from about 0.5 to 20 L<sup>-1</sup>, where, until 1530 LT, for freezing temperatures of -20°C numbers are about 0.6 L<sup>-1</sup>, except for a short period around 1400 LT which coincided with an increase in wind speed (Fig. ES3). From 1530 LT, INP number concentrations at -26°C increased to about 10 L<sup>-1</sup>. The DeMott et al. (2010) parameterization slightly over and underestimated INP number concentrations for higher and lower freezing temperatures, respectively, as in the case for PINE-c but yielded agreement within uncertainties of the CFDC measurement. For the most part, the INAS parameterization, dominated by mineral dust INPs, captured the observations within uncertainties with the trend to overestimate INP number concentrations. Since the CFDC has a lower cutoff size compared to PINE-c (2.5 versus 5 μm), biological INPs might not impact closure calculations as significantly as for PINE-c (assuming the biological particles are in the larger size class). If all particles are assumed to be dust INPs, similar to the case of the afternoon PINE-c measurements, INPs are further overpredicted, implying that either soil-organic INPs were not described correctly or the parameterization failed to capture the particular INP-type contributions for this scenario. The ABIFM parameterization, dominated by dust INPs, as in the case of INAS, generally underpredicted observed INP number concentrations and in some instances achieved agreement within uncertainties. Assuming all particles act as dust INPs, thus implying the presence of soil-organic INPs that mimic those parameterized by DD, ABIFM achieves good agreement with observations. This contrasts with INAS, and emphasizes the importance of potentially missing INPs (Fig. ES15) and the choice of parameterization. It is interesting to note that none of the immersion freezing parameterizations captured the change of

## Atmospheric ice-nucleating particles

Atmospheric ice formation has long been a fascination of the fundamental sciences, with profound implications for cloud properties and precipitation. Around the beginning of the twentieth century, balloon measurements indicated the presence of ice crystals that must have formed at supercooled temperatures higher than needed for the freezing of pure liquid water droplets as determined by Fahrenheit in 1724. At the same time, it was recognized that airborne dust particles are involved in ice formation, implying that insoluble particles can initiate ice nucleation. Those early observations revealed that only relatively few atmospheric dust particles act as INPs. Over 100 years later, we still face the conundrum of understanding which of the atmospheric particles initiate ice crystal formation. This aerosol–ice formation closure pilot study takes up the challenge of evaluating our predictive understanding of INPs in an air mass. We now know that ice forms via different nucleation modes, each with its own dependencies on particle type and atmospheric temperature and supersaturation. The major modes include immersion freezing where an INP is first immersed in a supercooled water droplet, deposition nucleation where ice forms upon deposition from the supersaturated gas phase, and contact freezing where an INP collides with a supercooled water droplet. In addition to these so-called primary ice formation processes, secondary ice production mechanisms, potentially involving collisions of preexisting ice particles with other hydrometeors and ice fracturing, can lead to substantial additional ice crystal formation. Constraining the primary ice nucleation mechanisms is crucial for prediction of atmospheric ice formation and, thus, climate and the hydrological cycle. Around the 1950s, Fletcher developed a theory of heterogeneous ice nucleation describing the energy requirement and rate coefficients of the formation of a critical ice germ on an insoluble substrate. Based on empirical results, he also derived an approximation that the number of INPs depends exponentially on the degree of supercooling. These two approaches still reverberate in today's atmospheric ice nucleation community, where laboratory freezing data are either analyzed using theoretical models or with empirically based simplification. Field and laboratory ice nucleation studies indicate that more and/or larger particles result in greater freezing rates. This is because a larger total particle surface area translates to a greater chance of the presence of ice nucleating particle features. Thus, it is commonly assumed that INPs are larger in size compared to cloud condensation nuclei. The last 20 years have seen an outburst of ice nucleation studies, examining numerous particle types for their abilities to serve as INPs, as well as new instrumentation development. That work now provides a basis for this aerosol–ice formation closure study in which we evaluate our ability to predict the number concentration of those enigmatic INPs entirely from the physical and chemical characteristics of an ambient particle population. By predicting ice formation from ambient aerosol, a key task in today's most advanced Earth system models, this exercise provides a pathway to improve their representation of ice crystal formation.

INP number concentrations at 1430 LT. There was no difference in the observed PSDs during this time period and as such we speculate that different types of INPs, not captured by the closure calculation, entered the CFDC.

In summary, the morning INP number concentrations were best described by the DeMott et al. (2010) parameterization that does not consider particle composition but is derived from field measurements. Particle composition specific parameterizations slightly underestimated morning INP number concentrations. This is likely due to missing INP types associated with organic material (secondary or soil derived) or the inapplicability of published parameterizations for INPs at this site. In the afternoon, every INP parameterization achieved some degree of closure for different reasons. In general, considering that offline INP measurements indicate the presence of INPs not captured in applied parameterized INP types, such as soil-organic and biological particles, one would expect an underestimation of INP number concentrations. This behavior was captured by ABIFM, thereby, in instances predicting too little INP number concentration. This clearly emphasizes that more efforts are needed to resolve the underlying parameters that govern immersion freezing.

### **What has been learned from this first closure exercise?**

Considering that we have so far only examined one day for this closure exercise, this first investigation has already provided valuable insight about the best strategies for examining immersion freezing from ambient particles and how to improve prediction of INP number concentrations. However, it is too premature to make final conclusions about our predictive capability for atmospheric immersion freezing. Keeping this in mind, we answer our research objectives in Table 1 with the analyses done so far.

**Overall objective.** It is too early to determine the most “robust” immersion freezing parameterization from one closure exercise. However, the results strongly suggest that if the ambient aerosol population is well characterized in terms of size distribution and particle types, INP number concentrations can be predicted from aerosol particle properties when immersion freezing parameterizations are available. The ice nucleation community’s recent efforts determining immersion freezing data in laboratory and field experiments made this advancement possible.

For the morning of the 15 October case, composition-specific immersion freezing parameterizations did not satisfactorily yield observed INP number concentrations; however, a parameterization derived from field observations performed better. This suggests that we are missing the immersion freezing ability of particle types such as mixed inorganic–organic particles and soil organics. As soon as freezing data for those particle types are established, closure can likely be more satisfactorily achieved for this specific case. For the afternoon, where the identified particle types were much better represented by existing immersion freezing parameterizations, partial and full closure was achieved by INAS and ABIFM, considering the lack of inclusion of soil-organic and biological INP types. Therefore, careful laboratory immersion freezing experiments involving inorganic–organic, soil-organic, and biological particles (and fragments thereof), are needed to improve closure for the discussed cases. However, field studies are equally important to isolate INP types as demonstrated in this study where soil-organic and biological particles emerge as potential INPs not yet sufficiently characterized and lacking in our closure calculations. Immersion freezing parameterizations derived from laboratory and field measurements still exhibit uncertainties, though the last 10 years have seen great improvement in the reproducibility of measured ice nucleation data. The reasons for this are manifold as discussed in recent intercomparison studies (DeMott et al. 2018; Hiranuma et al. 2015) and in analyses of the role of the uncertainties in particle surface area and freezing statistics (Alpert and Knopf 2016; Hartmann et al. 2016; Knopf et al. 2020).



**Research question 1:** The advancement of our predictive capability for atmospheric immersion freezing is greatly assisted by size-resolved aerosol composition analysis, including the coarse mode and refractory particles, and accompanying INP measurements. This includes improved speciation of the organic species (e.g., secondary, soil, biological macromolecules) and mineral dust types and efficiency in the analysis of larger sized particles. This approach will elucidate sources of bias in immersion freezing parameterizations.

**Research question 2:** This closure exercise suggests that surface area PSD and the size-resolved major particle types are sufficient (depending on location, 1–3 particle types may be enough) to achieve closure within measurement and parameterization uncertainties if corresponding immersion freezing parameterizations are available.

**Research question 3:** Our analysis suggests that for any meaningful INP number concentration predictions by models, the aerosol fields (PSD and composition) have to be sufficiently accurate to apply available immersion freezing parameterizations. The afternoon closure exercise (Figs. 6 and 7) suggests that INP number concentrations predicted by the climate model using INAS DD (Fig. 1) should have been in closer agreement with observations (even in the absence of soil-organic and biological INPs) in contrast to climate model predictions. One reason for this is likely the fact that mineral dust concentrations in the model are underestimated.

Overall, the advances in our understanding of immersion freezing garnered over the last 20 years are very promising to yield closure of atmospheric immersion freezing from ambient aerosol particles. However, when the aerosol population is physicochemically complex and parameterizations for representative INP types are not yet available, we still struggle to accurately predict INP number concentrations. With more laboratory and field measurements that are accompanied by particle composition analysis, the necessary datasets to achieve aerosol–ice formation closure for various locations will emerge, thus providing a robust foundation for guiding the representation of INPs in cloud and climate models.

**Acknowledgments.** This study was supported by the Atmospheric System Research Program and Atmospheric Radiation Measurement Program sponsored by the U.S. Department of Energy (DOE), Office of Science, Office of Biological and Environmental Research (OBER), Climate and Environmental Sciences Division (CESD), Award DE-SC0020006. DAK and PW acknowledge additional support under Award DE-SC0021034. PJD, TCJH, and JMC acknowledge additional support under Award DE-SC0018929. FRA, JMT, KAJ, RCM and AL acknowledge additional support under Award DE-SC0018948. NH and HSKV acknowledge support under Award DE-SC0018979. XL and YS acknowledge support under Award DE-SC0020510. NR and MW acknowledge funding from Award DE-SC0019192. AMF acknowledges support under Award DE-SC0016237 and from the NASA Radiation Science, and Modeling, Analysis and Prediction Programs. RCS, LGJ, and TAB acknowledge additional support from the National Science Foundation (CHE1554941, CBET1804737). KAM was supported by an NSF Graduate Research Fellowship under Grant 006784. Any opinions, findings, and conclusions or recommendations expressed in this material are those of the author(s) and do not necessarily reflect the views of the National Science Foundation. The PINE-c contribution is in part based upon work supported by the U.S. DOE Office of Science, OBER under Award DE-SC0018979. NH, HSKV, and KAS acknowledge Drs. Ottmar Möhler and Larissa Lacher for useful discussion regarding the PINE-c operation and associated data analysis. NH also thanks WT Office of Information Technology for technical support on remote PINE-c operation. Data were obtained from the Atmospheric Radiation Measurement (ARM) user facility, a U.S. DOE Office of Science user facility managed by the Biological and Environmental Research Program. The CCSEM/EDX particle analysis was performed in the Environmental Molecular Sciences Laboratory, a national scientific user facility sponsored by OBER at Pacific Northwest National Laboratory (PNNL). The STXM/NEXAFS particle analysis was performed at beamlines 11.0.2 and 5.3.2.2

at the Advanced Light Source (ALS) at Lawrence Berkeley National Laboratory. The work at the ALS was supported by the Director, Office of Science, Office of Basic Energy Sciences, of the U.S. DOE under Contract DE-AC02-05CH11231. We thank M. Marcus, H. Ohldag, and A.L.D. Kilcoyne for their assistance with the STXM experiments. We thank ARM SGP site staff for assisting with instrument set up.

**Data availability statement.** The data for this paper are available via the DOE ARM Data Archive and the closure calculation code is available upon request from the authors.

### Appendix: Instrumentation employed in aerosol–ice formation closure pilot study

This field campaign employed several online and offline instrumentation. Table A1 provides an overview of the instrumentation, including brief information on the examined particle size range, sample amount, and sampling frequency.

**Table A1. Atmospheric Radiation Measurement (ARM) site and guest instrumentation, online and offline, for physicochemical characterization of aerosol population and measurement of ice-nucleating particles. PSD refers to particle size distribution.**

Investigator	Instruments/methods	Measurement	Particle size range	Sampling rate	Measurement frequency
<b>Online</b>					
ARM Site	Scanning mobility particle sizer (SMPS)	PSD	~0.01–0.8- $\mu\text{m}$ diameter	0.1–0.3 LPM (liters per minute)	5 min
ARM Site	Aerodynamic particle sizer (APS)	PSD	~0.5–20- $\mu\text{m}$ diameter	5 LPM	1 s
Colorado State University (CSU)	Continuous Flow Diffusion Chamber (CFDC) with alternating ambient concentrator	Immersion-mode INP concentration at $-15^\circ$ and $-30^\circ\text{C}$	Up to $\sim 2.5 \mu\text{m}$ , 50% cut point	1.5 LPM	Typically integrated 3–5 min
CSU	Wideband Integrated Bioaerosol Sensor (WIBS model 4A)	Fluorescence and PSD of biological particles	~0.5–20 $\mu\text{m}$	0.3 LPM	Continuous
Carnegie Mellon University (CMU)	SMPS	PSD	~0.01–0.8- $\mu\text{m}$ diameter	0.3 LPM	4 min
CMU	APS	PSD	~0.5–20- $\mu\text{m}$ diameter	5 LPM	1 s
CMU	Laser Ablation Aerosol Particle Time-of-Flight Mass Spectrometer (LAAPTOF)	Size-distributed single-particle aerosol composition/type	0.2–3 $\mu\text{m}$	0.1 LPM	30 min
CMU	Soot-Particle Aerosol Mass Spectrometer (SP-AMS)	Size-distributed single-particle aerosol composition/type	0.05–0.8 $\mu\text{m}$	0.1 LPM	4 min
West Texas A&M University (WTAMU)	Portable Ice Nucleation Experiment chamber (PINE-c)	Immersion-mode INP concentration at $-15^\circ$ and $-30^\circ\text{C}$	0.35–5 $\mu\text{m}$	2–5 LPM	5 min
<b>Offline</b>					
Stony Brook University/Purdue University (SBU/PU)	Aerosol collection by multi orifice uniform deposition impaction (MOUDI)	Size distributed aerosol composition/type of aerosol	0.15–16 $\mu\text{m}$	30 LPM	1–4 h
SBU	Multi Orifice Uniform Deposition Impaction Droplet Freezing Technique (MOUDI-DFT)	INP concentration, frozen fraction	0.15–16 $\mu\text{m}$	30 LPM	1–4 h
CSU	Davis Rotating-drum Unit for Monitoring coupled with a Cold Plate (DRUM-CP) for size-resolved bulk immersion freezing	INP concentration, frozen fraction	0.13–12 $\mu\text{m}$	26–30 LPM	24 h
CMU	Microfluidic Ice Nucleation Technique (MINT)	INP concentration, frozen fraction	All into filter	16–18 LPM	4+ h
CSU	Ice Spectrometer (IS) for bulk immersion freezing with heat labile and organic INP analyses	INP concentration, frozen fraction	All into filter	16–18 LPM	1–4 h

## References

- Alpert, P. A., and D. A. Knopf, 2016: Analysis of isothermal and cooling-rate-dependent immersion freezing by a unifying stochastic ice nucleation model. *Atmos. Chem. Phys.*, **16**, 2083–2107, <https://doi.org/10.5194/acp-16-2083-2016>.
- Ansmann, A., and Coauthors, 2009: Dust and smoke transport from Africa to South America: Lidar profiling over Cape Verde and the Amazon rainforest. *Geophys. Res. Lett.*, **36**, L11802, <https://doi.org/10.1029/2009GL037923>.
- Augustin-Bauditz, S., and Coauthors, 2016: Laboratory-generated mixtures of mineral dust particles with biological substances: Characterization of the particle mixing state and immersion freezing behavior. *Atmos. Chem. Phys.*, **16**, 5531–5543, <https://doi.org/10.5194/acp-16-5531-2016>.
- Berkemeier, T., M. Shiraiwa, U. Pöschl, and T. Koop, 2014: Competition between water uptake and ice nucleation by glassy organic aerosol particles. *Atmos. Chem. Phys.*, **14**, 12 513–12 531, <https://doi.org/10.5194/acp-14-12513-2014>.
- Beydoun, H., M. Polen, and R. C. Sullivan, 2016: Effect of particle surface area on ice active site densities retrieved from droplet freezing spectra. *Atmos. Chem. Phys.*, **16**, 13 359–13 378, <https://doi.org/10.5194/acp-16-13359-2016>.
- Boucher, O., and Coauthors, 2013: Clouds and aerosols. *Climate Change 2013: The Physical Science Basis*, T. F. Stocker et al., Eds., Cambridge University Press, 571–657.
- Burkert-Kohn, M., and Coauthors, 2017: Leipzig Ice Nucleation Chamber Comparison (LINC): Intercomparison of four online ice nucleation counters. *Atmos. Chem. Phys.*, **17**, 11 683–11 705, <https://doi.org/10.5194/acp-17-11683-2017>.
- Charnawskas, J. C., and Coauthors, 2017: Condensed-phase biogenic–anthropogenic interactions with implications for cold cloud formation. *Faraday Discuss.*, **200**, 164–195, <https://doi.org/10.1039/C7FD00010C>.
- China, S., and Coauthors, 2017: Ice cloud formation potential by free tropospheric particles from long-range transport over the northern Atlantic Ocean. *J. Geophys. Res. Atmos.*, **122**, 3065–3079, <https://doi.org/10.1002/2016JD025817>.
- Connolly, P. J., O. Möhler, P. R. Field, H. Saathoff, R. Burgess, T. Choularton, and M. Gallagher, 2009: Studies of heterogeneous freezing by three different desert dust samples. *Atmos. Chem. Phys.*, **9**, 2805–2824, <https://doi.org/10.5194/acp-9-2805-2009>.
- Cziczo, D. J., and Coauthors, 2017: Measurements of ice nucleating particles and ice residuals. *Ice Formation and Evolution in Clouds and Precipitation: Measurement and Modeling Challenges*, Meteor. Monogr., Amer. Meteor. Soc., <https://doi.org/10.1175/AMSMONOGRAPHSD-16-0008.1>.
- de Boer, G., H. Morrison, M. D. Shupe, and R. Hildner, 2011: Evidence of liquid dependent ice nucleation in high-latitude stratiform clouds from surface remote sensors. *Geophys. Res. Lett.*, **38**, L01803, <https://doi.org/10.1029/2010GL046016>.
- DeMott, P. J., 1990: An exploratory study of ice nucleation by soot aerosols. *J. Appl. Meteor.*, **29**, 1072–1079, [https://doi.org/10.1175/1520-0450\(1990\)029<1072:AESOIN>2.0.CO;2](https://doi.org/10.1175/1520-0450(1990)029<1072:AESOIN>2.0.CO;2).
- , and Coauthors, 2010: Predicting global atmospheric ice nuclei distributions and their impacts on climate. *Proc. Natl. Acad. Sci. USA*, **107**, 11 217–11 222, <https://doi.org/10.1073/pnas.0910818107>.
- , and Coauthors, 2011: Resurgence in ice nuclei measurement research. *Bull. Amer. Meteor. Soc.*, **92**, 1623–1635, <https://doi.org/10.1175/2011BAMS3119.1>.
- , and Coauthors, 2015: Integrating laboratory and field data to quantify the immersion freezing ice nucleation activity of mineral dust particles. *Atmos. Chem. Phys.*, **15**, 393–409, <https://doi.org/10.5194/acp-15-393-2015>.
- , and Coauthors, 2017: Comparative measurements of ambient atmospheric concentrations of ice nucleating particles using multiple immersion freezing methods and a continuous flow diffusion chamber. *Atmos. Chem. Phys.*, **17**, 11 227–11 245, <https://doi.org/10.5194/acp-17-11227-2017>.
- , and Coauthors, 2018: The Fifth International Workshop on Ice Nucleation phase 2 (FIN-02): Laboratory intercomparison of ice nucleation measurements. *Atmos. Meas. Tech.*, **11**, 6231–6257, <https://doi.org/10.5194/amt-11-6231-2018>.
- Gelaro, R., and Coauthors, 2017: The Modern-Era Retrospective Analysis for Research and Applications, version 2 (MERRA-2). *J. Climate*, **30**, 5419–5454, <https://doi.org/10.1175/JCLI-D-16-0758.1>.
- Haag, W., B. Kärcher, J. Strom, A. Minikin, U. Lohmann, J. Ovarlez, and A. Stohl, 2003: Freezing thresholds and cirrus cloud formation mechanisms inferred from in situ measurements of relative humidity. *Atmos. Chem. Phys.*, **3**, 1791–1806, <https://doi.org/10.5194/acp-3-1791-2003>.
- Hartmann, S., H. Wex, T. Clauss, S. Augustin-Bauditz, D. Niedermeier, M. Rosch, and F. Stratmann, 2016: Immersion freezing of kaolinite: Scaling with particle surface area. *J. Atmos. Sci.*, **73**, 263–278, <https://doi.org/10.1175/JAS-D-15-0057.1>.
- Heymsfield, A. J., L. M. Miloshevich, C. Twohy, G. Sachse, and S. Oltmans, 1998: Upper-tropospheric relative humidity observations and implications for cirrus ice nucleation. *Geophys. Res. Lett.*, **25**, 1343–1346, <https://doi.org/10.1029/98GL01089>.
- Hiranuma, N., and Coauthors, 2015: A comprehensive laboratory study on the immersion freezing behavior of illite NX particles: A comparison of 17 ice nucleation measurement techniques. *Atmos. Chem. Phys.*, **15**, 2489–2518, <https://doi.org/10.5194/acp-15-2489-2015>.
- , and Coauthors, 2019: A comprehensive characterization of ice nucleation by three different types of cellulose particles immersed in water. *Atmos. Chem. Phys.*, **19**, 4823–4849, <https://doi.org/10.5194/acp-19-4823-2019>.
- Hoose, C., and O. Möhler, 2012: Heterogeneous ice nucleation on atmospheric aerosols: A review of results from laboratory experiments. *Atmos. Chem. Phys.*, **12**, 9817–9854, <https://doi.org/10.5194/acp-12-9817-2012>.
- Hopkins, R. J., A. V. Tivanski, B. D. Marten, and M. K. Gilles, 2007: Chemical bonding and structure of black carbon reference materials and individual carbonaceous atmospheric aerosols. *J. Aerosol Sci.*, **38**, 573–591, <https://doi.org/10.1016/j.jaerosci.2007.03.009>.
- Kanji, Z. A., O. Florea, and J. P. D. Abbatt, 2008: Ice formation via deposition nucleation on mineral dust and organics: Dependence of onset relative humidity on total particulate surface area. *Environ. Res. Lett.*, **3**, 025004, <https://doi.org/10.1088/1748-9326/3/2/025004>.
- , L. A. Ladino, H. Wex, Y. Boose, M. Burkert-Kohn, D. J. Cziczo, and M. Krämer, 2017: Overview of ice nucleating particles. *Ice Formation and Evolution in Clouds and Precipitation: Measurement and Modeling Challenges*, Geophys. Monogr., Amer. Meteor. Soc., <https://doi.org/10.1175/AMSMONOGRAPHSD-16-0006.1>.
- , and Coauthors, 2019: Heterogeneous ice nucleation properties of natural desert dust particles coated with a surrogate of secondary organic aerosol. *Atmos. Chem. Phys.*, **19**, 5091–5110, <https://doi.org/10.5194/acp-19-5091-2019>.
- , A. Welti, J. C. Corbin, and A. A. Mensah, 2020: Black carbon particles do not matter for immersion mode ice nucleation. *Geophys. Res. Lett.*, **47**, e2019GL086764, <https://doi.org/10.1029/2019GL086764>.
- Khlystov, A., C. Stanier, and S. N. Pandis, 2004: An algorithm for combining electrical mobility and aerodynamic size distributions data when measuring ambient aerosol. *Aerosol Sci. Technol.*, **38** (Suppl.), 229–238, <https://doi.org/10.1080/02786820390229543>.
- Knopf, D. A., and P. A. Alpert, 2013: A water activity based model of heterogeneous ice nucleation kinetics for freezing of water and aqueous solution droplets. *Faraday Discuss.*, **165**, 513–534, <https://doi.org/10.1039/c3fd00035d>.
- , and Coauthors, 2014: Microspectroscopic imaging and characterization of individually identified ice nucleating particles from a case field study. *J. Geophys. Res. Atmos.*, **119**, 10 365–10 381, <https://doi.org/10.1002/2014JD021866>.
- , P. A. Alpert, and B. Wang, 2018: The role of organic aerosol in atmospheric ice nucleation: A review. *ACS Earth Space Chem.*, **2**, 168–202, <https://doi.org/10.1021/acsearthspacechem.7b00120>.
- , —, A. Zipori, N. Reicher, and Y. Rudich, 2020: Stochastic nucleation processes and substrate abundance explain time-dependent freezing in supercooled droplets. *npj Climate Atmos. Sci.*, **3**, 2, <https://doi.org/10.1038/s41612-020-0106-4>.

- Moffet, R. C., A. V. Tivanski, and M. K. Gilles, 2010a: Scanning X-ray transmission microscopy: Applications in atmospheric aerosol research. *Fundamentals and Applications in Aerosol Spectroscopy*, R. Signorell and J. P. Reid, Eds., Taylor and Francis, 419–462.
- , T. Henn, A. Laskin, and M. K. Gilles, 2010b: Automated chemical analysis of internally mixed aerosol particles using X-ray spectromicroscopy at the carbon K-edge. *Anal. Chem.*, **82**, 7906–7914, <https://doi.org/10.1021/ac1012909>.
- Möhler, O., and Coauthors, 2008: The effect of organic coating on the heterogeneous ice nucleation efficiency of mineral dust aerosols. *Environ. Res. Lett.*, **3**, 025007, <https://doi.org/10.1088/1748-9326/3/2/025007>.
- Murray, B. J., D. O'Sullivan, J. D. Atkinson, and M. E. Webb, 2012: Ice nucleation by particles immersed in supercooled cloud droplets. *Chem. Soc. Rev.*, **41**, 6519–6554, <https://doi.org/10.1039/c2cs35200a>.
- Niemand, M., and Coauthors, 2012: A particle-surface-area-based parameterization of immersion freezing on desert dust particles. *J. Atmos. Sci.*, **69**, 3077–3092, <https://doi.org/10.1175/JAS-D-11-0249.1>.
- O'Sullivan, D., B. J. Murray, J. F. Ross, and M. E. Webb, 2016: The adsorption of fungal ice-nucleating proteins on mineral dusts: A terrestrial reservoir of atmospheric ice-nucleating particles. *Atmos. Chem. Phys.*, **16**, 7879–7887, <https://doi.org/10.5194/acp-16-7879-2016>.
- Ovchinnikov, M., and Coauthors, 2014: Intercomparison of large-eddy simulations of Arctic mixed-phase clouds: Importance of ice size distribution assumptions. *J. Adv. Model. Earth Syst.*, **6**, 223–248, <https://doi.org/10.1002/2013MS000282>.
- Pruppacher, H., R., and J. D. Klett, 1997: *Microphysics of Clouds and Precipitation*. 2nd ed. Kluwer Academic, 954 pp.
- Quinn, P. K., and D. J. Coffman, 1998: Local closure during the First Aerosol Characterization Experiment (ACE 1): Aerosol mass concentration and scattering and backscattering coefficients. *J. Geophys. Res.*, **103**, 16 575–16 596, <https://doi.org/10.1029/97JD03757>.
- Rigg, Y. J., P. A. Alpert, and D. A. Knopf, 2013: Immersion freezing of water and aqueous ammonium sulfate droplets initiated by humic-like substances as a function of water activity. *Atmos. Chem. Phys.*, **13**, 6603–6622, <https://doi.org/10.5194/acp-13-6603-2013>.
- Schill, G. P., and Coauthors, 2020: The contribution of black carbon to global ice nucleating particle concentrations relevant to mixed-phase clouds. *Proc. Natl. Acad. Sci. USA*, **117**, 22 705–22 711, <https://doi.org/10.1073/pnas.2001674117>.
- Seifert, M., and Coauthors, 2004: Thermal stability analysis of particles incorporated in cirrus crystals and of non-activated particles in between the cirrus crystals: Comparing clean and polluted air masses. *Atmos. Chem. Phys.*, **4**, 1343–1353, <https://doi.org/10.5194/acp-4-1343-2004>.
- Stein, A. F., R. R. Draxler, G. D. Rolph, B. J. B. Stunder, M. D. Cohen, and F. Ngan, 2015: NOAA's HYSPLIT atmospheric transport and dispersion modeling system. *Bull. Amer. Meteor. Soc.*, **96**, 2059–2077, <https://doi.org/10.1175/BAMS-D-14-00110.1>.
- Sullivan, R. C., L. Minambres, P. J. DeMott, A. J. Prenni, C. M. Carrico, E. J. T. Levin, and S. M. Kreidenweis, 2010: Chemical processing does not always impair heterogeneous ice nucleation of mineral dust particles. *Geophys. Res. Lett.*, **37**, L24805, <https://doi.org/10.1029/2010GL045540>.
- Tan, I., T. Storelvmo, and M. D. Zelinka, 2016: Observational constraints on mixed-phase clouds imply higher climate sensitivity. *Science*, **352**, 224–227, <https://doi.org/10.1126/science.aad5300>.
- Thompson, S. K., 1987: Sample-size for estimating multinomial proportions. *Amer. Stat.*, **41**, 42–46.
- Tobo, Y., P. J. DeMott, T. C. J. Hill, A. J. Prenni, N. G. Swoboda-Colberg, G. D. Franc, and S. M. Kreidenweis, 2014: Organic matter matters for ice nuclei of agricultural soil origin. *Atmos. Chem. Phys.*, **14**, 8521–8531, <https://doi.org/10.5194/acp-14-8521-2014>.
- Vali, G., P. J. DeMott, O. Möhler, and T. F. Whale, 2015: A proposal for ice nucleation terminology. *Atmos. Chem. Phys.*, **15**, 10 263–10 270, <https://doi.org/10.5194/acp-15-10263-2015>.
- VanReken, T. M., T. A. Rissman, G. C. Roberts, V. Varutbangkul, H. H. Jonsson, R. C. Flagan, and J. H. Seinfeld, 2003: Toward aerosol/cloud condensation nuclei (CCN) closure during CRYSTAL-FACE. *J. Geophys. Res.*, **108**, 4633, <https://doi.org/10.1029/2003JD003582>.
- von der Weiden, S. L., F. Drewnick, and S. Borrmann, 2009: Particle Loss Calculator—A new software tool for the assessment of the performance of aerosol inlet systems. *Atmos. Meas. Tech.*, **2**, 479–494, <https://doi.org/10.5194/amt-2-479-2009>.
- Wang, B., and D. A. Knopf, 2011: Heterogeneous ice nucleation on particles composed of humic-like substances impacted by O<sub>3</sub>. *J. Geophys. Res.*, **116**, D03205, <https://doi.org/10.1029/2010JD014964>.
- , A. Laskin, T. Roedel, M. K. Gilles, R. C. Moffet, A. V. Tivanski, and D. A. Knopf, 2012a: Heterogeneous ice nucleation and water uptake by field-collected atmospheric particles below 273 K. *J. Geophys. Res.*, **117**, D00V19, <https://doi.org/10.1029/2012JD017446>.
- , A. T. Lambe, P. Massoli, T. B. Onasch, P. Davidovits, D. R. Worsnop, and D. A. Knopf, 2012b: The deposition ice nucleation and immersion freezing potential of amorphous secondary organic aerosol: Pathways for ice and mixed-phase cloud formation. *J. Geophys. Res.*, **117**, D16209, <https://doi.org/10.1029/2012JD018063>.
- Westbrook, C. D., and A. J. Illingworth, 2013: The formation of ice in a long-lived supercooled layer cloud. *Quart. J. Roy. Meteor. Soc.*, **139**, 2209–2221, <https://doi.org/10.1002/qj.2096>.
- Wolf, M. J., and Coauthors, 2020: A biogenic secondary organic aerosol source of cirrus ice nucleating particles. *Nat. Commun.*, **11**, 4834, <https://doi.org/10.1038/s41467-020-18424-6>.
- Zelinka, M. D., and Coauthors, 2020: Causes of higher climate sensitivity in CMIP6 models. *Geophys. Res. Lett.*, **47**, e2019GL085782, <https://doi.org/10.1029/2019GL085782>.